

MASS SPECTROSCOPY APPLIED TO  
GAS LEAK DETECTION AND FUEL IONIZATION

By

JAYANTH POTHIREDDY

A THESIS PRESENTED TO THE GRADUATE SCHOOL  
OF THE UNIVERSITY OF FLORIDA IN PARTIAL FULFILLMENT  
OF THE REQUIREMENTS FOR THE DEGREE OF  
MASTER OF SCIENCE

UNIVERSITY OF FLORIDA

2003

Copyright 2003

by

Jayanth Pothireddy

To my friends

## ACKNOWLEDGMENTS

I would like to sincerely thank Dr. Corin Segal for giving me this wonderful opportunity and for his unlimited support, understanding and incredible patience without which I would not have successfully completed my thesis. I would also like to thank Dr. David Mikolaitis and Dr. Martin Vala for their support and Dr. Norman Fitz-Coy for his valuable suggestions.

Many thanks go to Mr. Jan Szczepanski for giving me “first lessons” on mass spectrometry, invaluable suggestions, tremendous support and help in developing the mass spectrometry system.

My heartfelt thanks go to my friends Venkat, Sujith, Gopi, Anand, “Iranian bros” Amir and Omid, Weizhong, Sampath, Harsha, Adil, Anant, Sasidhar, Charan, Danny, Jonas, Nelson, Zhu Wei, Ron, “Dr” Amit, Errol, Anurag, Priya, Amit “Saale” and Balaji for their support and understanding.

I thank Ron Brown for constructing a nice model of the Space Shuttle aft compartment and for his help in moving the mass spectrometer cart to and fro from “chemistry” to “aero.”

## TABLE OF CONTENTS

	<u>Page</u>
ACKNOWLEDGMENTS.....	iv
LIST OF FIGURES.....	vii
ABSTRACT .....	ix
CHAPTERS	
1 INTRODUCTION.....	1
1.1 Introduction.....	1
1.2 Cryogenic Fuel Leaks .....	1
1.3 Ionization of Fuels .....	4
2 EXPERIMENTAL SETUP .....	9
2.1 Introduction.....	9
2.2 Aft-Compartment Model.....	9
2.3 Ionization Tube .....	11
2.4 Mass-Spectrometer.....	12
2.4.1 Ion Sources .....	14
2.4.2 Mass Analyzers.....	17
2.4.3 Detectors .....	18
2.5 The SRS Residual Gas Analyzer .....	19
2.5.1 Ionizer .....	20
2.5.2 Quadrupole Mass Filter: .....	21
2.5.3 Ion Detector .....	23
2.5.4 Modes of Operation of SRS RGA .....	24
2.6 Vacuum System .....	25
3 RESULTS AND SUMMARY .....	26
3.1 Introduction.....	26
3.2 Data Acquisition and Calibration.....	26
3.2 Leak Detection Tests.....	28
3.3 Ionization Tests .....	30
3.5 Summary .....	33

APPENDIX

A AFT COMPARTMENT MODEL ..... 35

B STANFORD RESEARCH SYSTEMS RESIDUAL GAS ANALYZER 300..... 39

    B.1 SRS Mass Spectrometer ..... 39

        B.1.1 Specifications ..... 39

        B.1.2 Internal Components ..... 40

    B.2 Electrostatic Ion Lens System ..... 41

LIST OF REFERENCES ..... 44

BIOGRAPHICAL SKETCH ..... 46

## LIST OF FIGURES

<u>Figure</u>	<u>page</u>
2-1. Aft compartment model- <i>left side view</i> . ....	11
2-2. Ionization tube. ....	12
2-3. Basic components of a mass spectrometer with feedback control carried by a computer. ....	13
2-4. SRS Mass spectrometer. ....	19
2-5. Ionizer Schematic. Reproduced from Ref. 4. ....	20
2-6. Quadrupole rod connections. Reproduced from Ref. 4. ....	21
2-7. Ion Detector Components. Reproduced from Ref. 4. ....	24
2-8. Vacuum pumping system. ....	25
3-1. Analog scans- mass scale calibration. ....	27
3-2. Helium leak detection concentration curve for $L=1.3\text{ cm}$ . ....	29
3-3. Helium leak detection concentration curve for $L=2.5\text{ cm}$ . ....	29
3-4. Butane ( $C_4H_{10}$ ) ionization. ....	31
3-4 (contd.). Butane ( $C_4H_{10}$ ) ionization. ....	32
3-5. Normalized fragmentation species pressure. ....	33
A-1. Hull. ....	35
A-2. Hull-front piece. ....	36
A-3. Hull- rear piece. ....	36
A-4. Hull- side piece. ....	37
A-5. Hull- shoulder piece. ....	37

A-6. Hull- top piece.....	38
A-7. Hull- bottom piece. ....	38
B-1. Ionizer Components. ....	40
B-2. Quadrupole Mass Filter Components.....	40
B-3. Electrostatic ion lens system. ....	41
B-4. ICP, ion sampling interface, and vacuum system. Reproduced from Ref. 21. ....	42
B-5. Schematic of SRS mass spectrometer with the electrostatic ion lens assembly for ionization studies. ....	43

Abstract of Thesis Presented to the Graduate School  
of the University of Florida in Partial Fulfillment of the  
Requirements for the Degree of Master of Science

MASS SPECTROSCOPY APPLIED TO  
GAS LEAK DETECTION AND FUEL IONIZATION

By

Jayanth Pothireddy

August 2003

Chair: Corin Segal

Major Department: Mechanical and Aerospace Engineering

A quadrupole mass spectrometry system was evaluated for two distinct applications: gas leak detection in a scaled model of the space shuttle aft compartment and to characterize the effect of fuel ionization. Stanford Research Systems Residual Gas Analyzer 300 was evaluated in this study.

The leak detection experiments were conducted by simulating He gas leaks for cryogenic fuel leaks, inside a model of the space shuttle aft compartment. For this study, He gas leak at a pressure of 241 *kPa* was initiated through a 1.6 *mm* tygon tube at six predetermined locations inside the aft compartment model. The air purge rate into the model was 0.012 SCMS. The mass spectrometer did not detect the presence of He in the model even after an hour of leak. The non-detection of leak by the SRS mass spectrometer might be that the amount of He leak initiated into the model was low at the conditions tested.

In the ionization studies, butane ( $C_4H_{10}$ ) gas was introduced into the SRS mass spectrometer bypassing the ionization tube. The effects of internal ionization on butane were studied at 25, 40 and 70 *eV* ionization potential (IP). The results showed increasing intensity and fragmentation of butane into smaller species with increasing IP. The study indicated the absence of methyl radical ( $CH_3^+$ ) for butane ionization at 25 *eV*. Also the study showed the inherent limitation of SRS mass spectrometer, that it cannot be operated without switching the filament ON. Hence, for the ionization studies using the SRS mass spectrometer system, the filament has to be physically isolated from the system to characterize the effect of external ionization in the ionization tube.

## CHAPTER 1 INTRODUCTION

### 1.1 Introduction

A gas analysis mass spectrometry system has been evaluated for two distinct applications: (1) a model of the space shuttle engine compartment to detect the presence of potentially explosive mixtures, and (2) high-speed gaseous hydrocarbons ionized to provide accelerated chemical reactions in a model scramjet. Gas composition detection with application to these issues are described, generally, in this section.

### 1.2 Cryogenic Fuel Leaks

The danger of a fire on the space shuttle can be generated by leak of fuel or oxidizer. The space shuttle main engines use liquid hydrogen (LH<sub>2</sub>) and liquid oxygen (LO<sub>2</sub>) as propellants. The cryogenic fuel, LH<sub>2</sub> and the oxidizer, LO<sub>2</sub> are stored in the external tank and fed to the main engines located in the aft compartment of the space shuttle during launch. A scaled model of the space shuttle aft compartment has been build and fuel leaks have been modeled at several locations. The current mass-spectrometer system is used to detect the spreading of this fuel throughout the compartment.

Mass-spectrometers have been used in the past to detect gas leaks in several applications. Griffin *et al.*<sup>1</sup> have noted that mass-spectrometry is the only technology proven to monitor all necessary gas constituents at the required limits of detection, as low as 25 parts-per-million by volume (ppmv). Traditionally, NASA used four mass-spectrometer based leak detection systems for each launch support: Prime Hazardous Gas

Detection System (HGDS), Backup HGDS, Portable Aft Mass Spectrometer<sup>2</sup> (PAMS), and Hydrogen Umbilical Mass Spectrometer (HUMS). NASA has introduced a new replacement system called the Hazardous Gas Detection System (HGDS) 2000 with new features including Multiple Detector Sample Delivery system, control of inlet pressure, use of an inexpensive quadrupole mass spectrometer, and new pumping technology. This system is capable of monitoring gas in helium, nitrogen, or air background and also enables near simultaneous monitoring of all gas constituents of interest. The system can detect the leaks of hydrogen and oxygen as low as 25 ppmv and argon concentrations as low as 10 ppmv, with a response time of less than 10 seconds.

Griffin *et al.*<sup>3</sup> reported the results of performance tests done to evaluate the Stanford Research Systems (SRS) RGA 100 quadrupole mass spectrometer for using as a detector subsystem on the HGDS 2000. It is mentioned that while the SRS mass spectrometer meets the needs for this system, no commercial mass spectrometer system was found to give the performance required. Accuracy, limits-of-detection, drift, response time (the time for the concentration reading to reach 95% of the actual value was taken as the response time), and recovery time (the time required for the concentration reading to measure within 5% of actual) of the system have been evaluated. For all the tests conducted, the SRS Residual Gas Analyzer<sup>4</sup> (RGA) was set to Noise Floor (NF) = 2 and mass-to-charges ( $m/z$ ) monitored were 2, 4, 32, and 40; and detector was Faraday Cup. Their tests showed that the RGA maintained good linearity and all the values fell within 10% of the readings. The response time was measured as 8 sec for each component and the recovery time was measured to be less than 20 sec except for H<sub>2</sub>, which was 2 min. It

was concluded that the mass spectrometer was the best method of leak detection for HGDS 2000.

The flammability limits of an oxygen and hydrogen mixture are an oxygen volume fraction  $\leq 4\%$  or a hydrogen volume fraction  $\leq 4\%$ . Altitude has little effect on the flammability limits of hydrogen and oxygen mixtures until altitudes above 80,000 feet.<sup>5, 6</sup>

Leak detection has a particular role in the evaluation of new composite materials based fuel tanks. New hydrogen tanks made of polymer-matrix composite (PMC) material are under consideration as an enabling technology for reducing the weight of reusable launch vehicles and increasing their payload. A key developmental issue for these lightweight structures has been the LH<sub>2</sub> leakage through the composite material. Rivers *et al.*<sup>7</sup> have developed a method to calibrate and measure the leakage through the X-33 liquid hydrogen tank at cryogenic temperatures and under mechanical loads. The Flexible Microleak Detection System (FMLDS) developed for the test uses a mass spectrometer to determine the leaks and rate of permeation in the event of low leak rates. The results reported indicate that the errors are less than 10% for leak rates ranging from 0.3 to 200 cm<sup>3</sup>/min.

A miniature quadrupole mass spectrometer array and gas chromatograph have been designed by Chutjian *et al.*<sup>8</sup> and built for NASA flight missions. The system is used for detection, by astronauts in EVA, of N<sub>2</sub>, O<sub>2</sub>, the hydrazines, and NH<sub>3</sub> leaks in the hull of the ISS, and of absorbed hydrazines on the astronauts' suits. Also the system will find use in long-duration human flight to monitor in the spacecraft the atmosphere, the quality of drinking water, and the microbial content of the air and surfaces.

Hunter *et al.*<sup>9</sup> discuss the needs of aeronautical and space applications and the point-contact sensor technology to address these needs. The method of leak detection currently used for the space shuttle is a mass-spectrometer connected to an array of sampling tubes placed throughout the region of interest. The device was able to detect hydrogen in a variety of ambient environments, but it had its drawbacks, delay time with leak detection and pinpointing the exact location of the leak.

### 1.3 Ionization of Fuels

In many practical devices such as ramjets experimental investigations have shown that there are serious difficulties concerning ignition of hydrocarbons due to relatively long times to initiate chemical reactions relative to the residence times. These problems are more predominant in time-limited combustion systems, in particular, supersonic combustion-based propulsion devices, where the fluid residence times may approach the chemical reaction rates. Therefore, methods are needed to accelerate the reactions to achieve stable and efficient energy deposition in the flow.

A possibility to increase the production of free radicals from hydrocarbon fuel is to ionize it. The ions are expected to contribute to the acceleration of chemical reactions. The degree of ionization and the ions production are evaluated via mass spectrometry. The main difference among the methods for plasma ionization lies in the form in which energy is delivered to the sample: electric current (glow discharge, spark), microwave-induced plasma (MIP), pulsed laser.<sup>10</sup> Duncan indicated the recent developments in ionic molecular species production and to study their spectroscopy. Also new ion production schemes and/or modified ion sources are discussed, as are various mass spectrometry configurations used for mass selection.<sup>11</sup>

Combustion systems benefit from the acceleration of chemical reactions to reduce the ignition delay time and to enhance the recombination reaction rates. Buriko *et al.*<sup>12</sup> in their studies have found that air-fuel reactivity can be increased by injecting additives that contain radicals in large concentration, or by generation of free radicals prior to injection through ionization. Also Buriko *et al.* indicated that the ignition delay time can be decreased by as much as 20% due to free radicals resulting from ionization of hydrocarbons:  $\text{CO}^-$ ,  $\text{H}^-$ ,  $\text{CH}_3^-$ ,  $\text{HCO}^-$ ,  $\text{CH}_2\text{O}^-$ ,  $\text{C}_3\text{H}_7^-$  etc., and over 50% when radicals containing atomic oxygen anion ( $\text{O}^-$ ) are present. These results coincide with other recent studies conducted by Williams *et al.*<sup>13</sup> which indicate that reactions can be accelerated when ions found in air plasmas react with aromatic fuel compounds typically found in aviation (JP) fuels.

Using experimental techniques and theoretical analyses, Arnold *et al.*<sup>14</sup> have conducted studies on gas-phase ion molecule reactions of the primary atmospheric cations ( $\text{NO}^+$ ,  $\text{O}_2^+$ ,  $\text{O}^+$ ,  $\text{N}^+$ , and  $\text{N}_2^+$ ) with two isomers of octane, *n*- $\text{C}_8\text{H}_{18}$  and *iso*- $\text{C}_8\text{H}_{18}$  (2,2,4-trimethylpentane). Reaction rate constants and branching ratios for the reactions were measured from 300 to 500 K. It is reported that the ion-molecule reaction rates are significantly faster and initiate radical formation at much lower temperatures.

Arnold *et al.*<sup>15</sup> have done extensive studies of the reactions of air plasma ions with a variety of alkanes. Especially the larger alkanes commonly found in fuels such as gasoline or kerosene, to explore the possibility that air plasma ions could be used as additives to enhance the rate of combustion of hydrocarbon fuels or to reduce the ignition delay time. They have shown that the positive ions  $\text{H}_3\text{O}^+$  and  $\text{NO}^+$ , which appear through the ionization of air (air plasma ions), have a significant effect on accelerating

the decomposition reactions of large alkane compounds, beginning with C<sub>6</sub> groups. This result is of particular interest for practical devices, such as aerospace vehicle engines, that employ mixtures of hydrocarbons of large C groups. Also the effects of these ions are influenced in different ways depending on the temperature at which these reactions take place. For example, the lower effectiveness of H<sub>3</sub>O<sup>+</sup>, which decomposes thermally between 300-400 K.

Arnold *et al.*<sup>16</sup> has studied reactions of atomic oxygen anion(O<sup>-</sup>) with a large number of alkanes. The efficiencies for the reactions of O<sup>-</sup> with ethane, propane, and butane increase with increasing size, becoming collisional for butane at room temperature. For pentane and larger alkanes, the reactions are collisional at all temperatures. Extending the studies, Arnold *et al.*<sup>17</sup> reported temperature dependence of reaction rates of the atmospheric plasma cations obtained from air ionization with benzene, a typical aromatic compound over a broad temperature range of 250 to 1400 K and the reactions were found to proceed at collisional rates.

In the past, gas-phase ion-molecule reactions up to 5 Torr were studied by flow tube experiments that were based on laminar flow dynamics. Arnold *et al.*<sup>18</sup> have developed a new instrument, the turbulent ion flow tube (TIFT), for studying ion-molecule reactions in the very high pressure range. It is designed to operate at room temperature and over a pressure range from approximately 20-750 Torr.

Williams *et al.*<sup>13</sup> reported the effect of air ions on other aromatic compounds, such as JP-10 (a synthetic high density compound), ethyl benzene and isooctane. The studies indicated a significant reduction in the ignition delay time, with stronger effects noted at low temperatures and large ionization levels. Possible explanations for the observed

effects are: (i) the ion-molecule reactions discussed are associated with high exothermicities, thus, the reduction of ignition delay time could be due to additional heat added to the system leading to an effective rise in temperature and thereby reducing the ignition delay time; (ii) the production of radicals initiated by the air-plasma chemistry followed by dissociative recombination of the resulting molecular ions could be responsible; (iii) reactions of the air-plasma ions with the fuel molecules result in the rapid decomposition of the initial constituents to smaller fuel fragments with lower ignition temperature.

Munson and Field presented a new technique in mass spectrometry called chemical ionization mass spectrometry.<sup>19</sup> This was based on the formation of the ions of an unknown material by chemical reactions in the gas phase. A reaction gas was introduced into the ionization chamber of a mass spectrometer that can produce a set of ions, which are either non-reactive or only very slightly reactive with the reaction gas itself at pressures of 1 *Torr*. When a small amount of another material is present in the mixture at these high pressures, the stable ions of the reaction gas will react with the second material to produce a spectrum of ions characteristic of the second material. It is reported that the spectra produced by this method are often more useful for determining the structure of compounds and identifying compounds and mixtures than electron impact spectra. Also the fragmentation patterns of chemical ionization mass spectrometry correspond closely to the structures of the molecules and appear to result from localized attack at reactive centers in the molecule.

Palmer *et al.*<sup>20</sup> gives a good description on the development and application of mass spectrometry instrumentation to support the goals of U.S. space program. The main

focus of the study is the application of MS in studying the composition of planetary atmospheres and monitoring air quality on manned space missions.

## CHAPTER 2 EXPERIMENTAL SETUP

### 2.1 Introduction

This chapter describes the experimental model for the leak detection, the ionization tube for ionization studies, the mass spectrometry theory, the description and working of SRS mass spectrometer and finally the vacuum pumping system.

### 2.2 Aft-Compartment Model

The Space Shuttle aft-compartment houses the main propulsion system: main engines, LO<sub>2</sub> and LH<sub>2</sub> feed lines, avionics bays, tanks, etc. A scaled, 1:4, Plexiglass (outer construction) geometric model of the space shuttle aft-compartment is constructed to include the following components inside the hull (*see* Figure 2-1):

1. The main LH<sub>2</sub> supply line connecting the interface with the external tank to hydrogen manifold. This is a 10.2 cm diameter line.
2. The 3 LH<sub>2</sub> lines connecting hydrogen manifold to the 3 main engines. These are 7.6 cm diameter lines.
3. The main LO<sub>2</sub> supply line connecting the interface with the external tank to the oxygen manifold which is a 10.2 cm diameter line.
4. The 3 LO<sub>2</sub> lines connecting the oxygen manifold to the 3 main engines, which are 7.6 cm diameter lines.
5. The hydrogen drain and fill lines. These are 5.1 cm diameter lines.
6. The oxygen drain and fill lines which are 5.1 cm diameter lines.
7. Three spherical hydrazine tanks which have a diameter of 17.8 cm.
8. Four spherical helium tanks which have a diameter of 15.3 cm.

9. Three boxes representing the avionics bay, two with  $35.6 \times 30.5 \times 26.6$  and one with  $35.5 \times 28.0 \times 20.3$  dimensions (cm).
10. Three cylinders with a length of 38.0 cm and diameter of 50.8 cm represent the main engines.

Table 2-1. Check Valve placement on the hull-front plate.

Check Valves	Co-ordinates [cm]	
	Y	Z
1	-23.8	134.2
2	23.8	134.2
3	-38.5	119.0
4	38.5	119.0
5	-10.9	99.5
6	18.3	76.4
7	-33.0	47.8
8	33.0	47.8
9	-47.3	8.4
10	-31.3	3.6
11	31.3	3.6
12	47.3	8.4
13	-26.7	17.9
14	26.7	17.9

The hull consists of flat-sided smooth outline planar figures and modeled without any structural frame members such as beams, trusses, etc. The purging of aft-compartment is done with air through the check valves placed on the hull front piece. The total purge flow rate was 0.012 SCMS. Table 2-1 gives the co-ordinates for the check-valve placement in the model co-ordinates. The hull ventilation is provided through four airtight hatches carved out on the hull- side and shoulder pieces.

The leak was initiated from a 16000 kPa industrial grade He gas cylinder at six predetermined locations inside the hull and sampling is done through six predetermined sample locations. He is used to simulate hydrogen gas leaks. The location of leak and sampling points are at manifold left (L1, S1), manifold right (L4, S4), bottom left (L2, S2), bottom right (L5, S5), side left (L3, S3) and side right (L6, S6). The leak and

sampling is done through a 1.3 mm tygon tube. The detailed model drawings are included in the Appendix A.

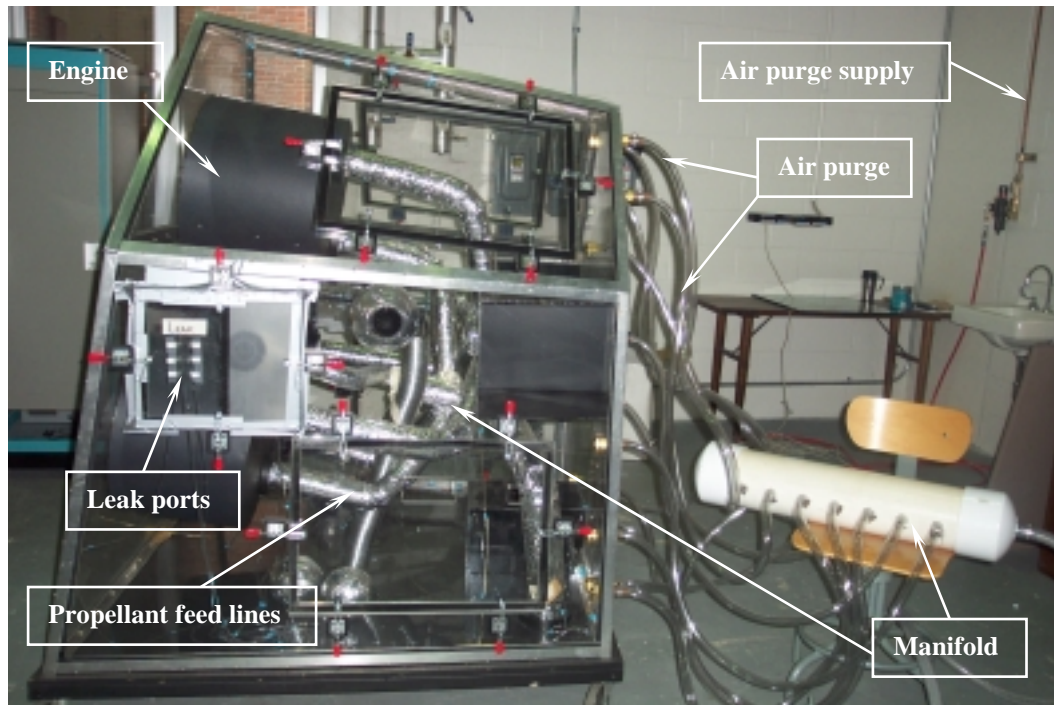


Figure 2-1. Aft compartment model- *left side view*.

### 2.3 Ionization Tube

The selected hydrocarbon gases have been ionized in the device shown in Figure 2-2. It has a glass tube with two circular electrodes at each end. The potential will be varied to obtain various degrees of ionization. The gases are ionized by the high dc potential of about 900 V applied between the two electrodes. The ionized gases are then directed into the mass spectrometer for measurements of ion production as a function of the ionization potential applied to the electrodes.

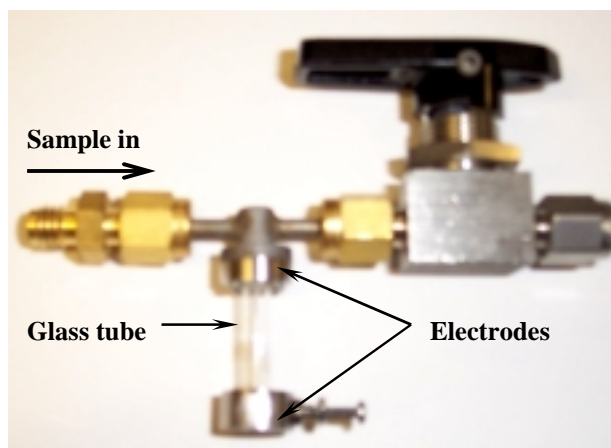
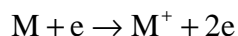


Figure 2-2. Ionization tube.

### 2.4 Mass-Spectrometer

The mass-spectrometer is an instrument that measures the masses of individual molecules that have been converted into ions, i.e., molecules that have been electrically charged. A mass-spectrometer does not actually measure the molecular mass directly, but rather measures the mass-to-charge ( $m/z$ ) ratio of the ions formed from the molecules. The mass spectrometry is a destructive technique and requires only a few nanomoles of sample to obtain its characteristic information.

The first step in the mass spectrometric analysis of compounds involves the production of gas-phase ions of the compound, e.g. by electron ionization:



This molecular ion may further undergo fragmentation giving new radical cations and neutral molecules. All these ions are separated in the mass-spectrometer according to their  $m/z$  ratio and are detected in proportion to their abundance.

Any typical mass spectrometer always contains the following functional units (*see* Figure 2-3):

1. A device to introduce the compound that is analyzed, e.g. a direct insertion probe or a gas chromatograph.
2. A source to produce ions from the sample.
3. An analyzer(s) to separate the various ions according to their  $m/z$  ratio.
4. A detector to count the ions emerging from the analyzer and to measure their abundance.
5. A computer to process the data, which produces the mass spectrum in a suitable form and controls the instrument through feedback.

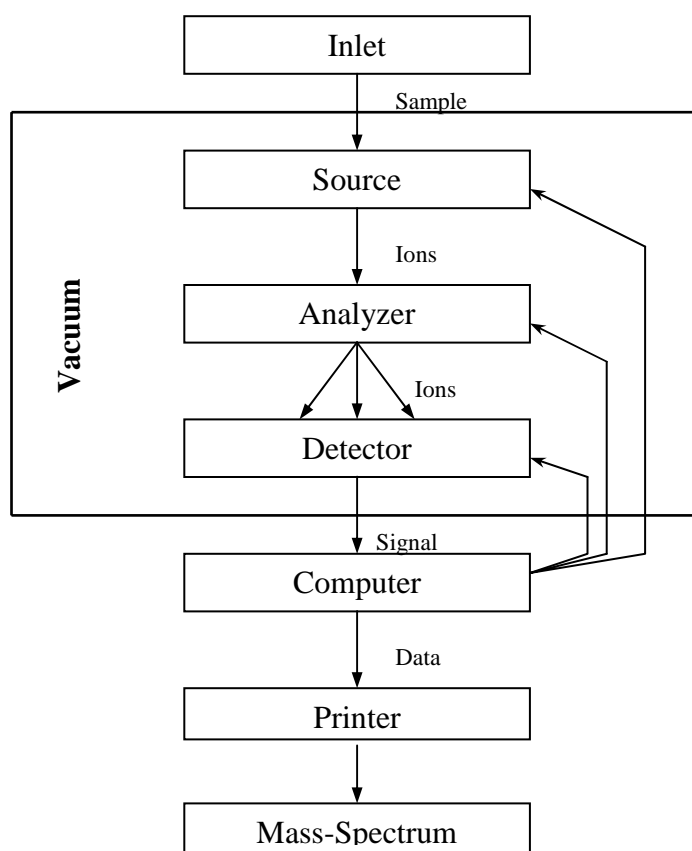
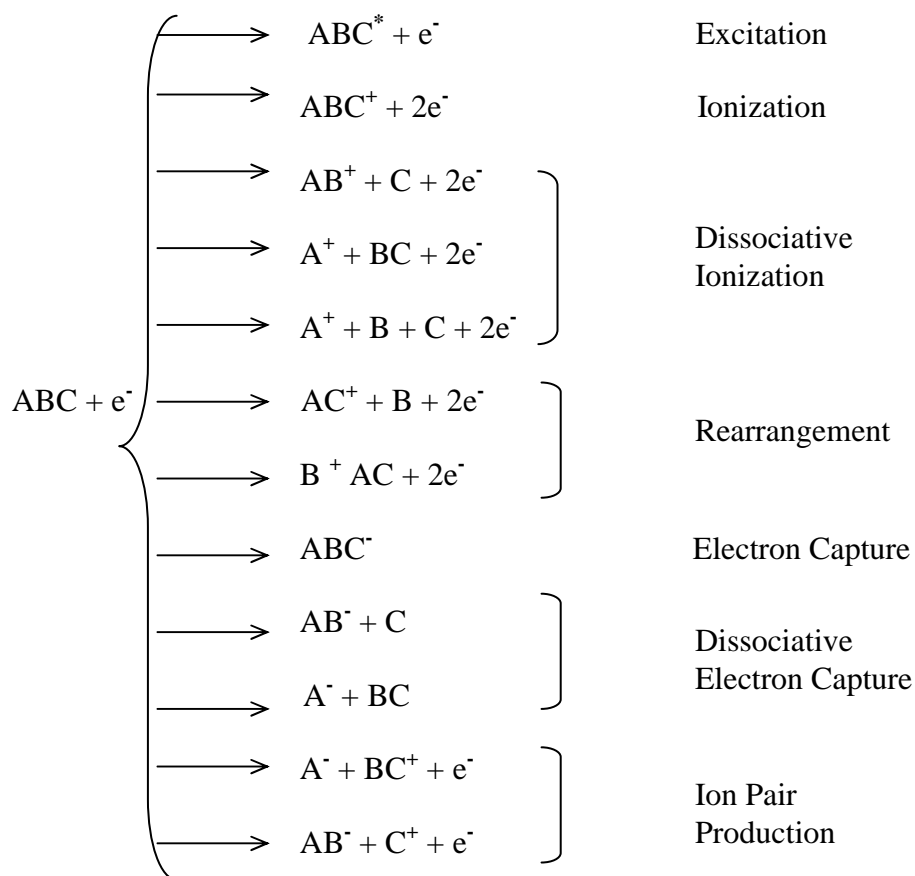


Figure 2-3. Basic components of a mass spectrometer with feedback control carried by a computer.

### 2.4.1 Ion Sources

Ion sources exist as two types: liquid-phase ion sources and solid-state ion sources. In a liquid-phase ion source the sample enters as solution. This solution is introduced, by nebulization, as droplets into the mass spectrometer through some vacuum pumping stages. Electrospray and thermospray correspond to this type. In a solid-state ion source the analyte is an involatile deposit. This deposit is irradiated by energetic particles or photons that desorb ions near the surface of the deposit. These ions can be extracted by an electric field and focussed on to the analyzer. Field desorption, plasma desorption and matrix-assisted laser desorption sources use this technique to produce ions.



The most important considerations applied while choosing a ionization technique are the internal energy transferred during ionization process and the physical and

chemical properties of the sample that has to be ionized. Some ionization techniques are very energetic and cause extensive fragmentation while others are less energetic and only produce molecular species. The ion sources produce ions mainly by ionizing a neutral molecule through electron ejection, electron capture, etc. Some ion source reactions were described in the previous page.

In *electron ionization* (EI) source, the sample is bombarded with a beam of energetic electrons. This ionization technique works well for many gas-phase molecules but induces extensive fragmentation so that the molecular ions are not always observed. This source consists of heated filament giving off electrons. These electrons are accelerated and made to collide with the gaseous molecules of the analyzed sample injected in to the source. Each electron is associated with an energy ( $eV$ ) given by,  $mv = h/\lambda$ , where  $m$  is its mass,  $v$  is its velocity,  $\lambda$  its wavelength and  $h$  is Planck's constant. Usually, the energy of the electron beam can be selected from about 25 to 100  $eV$  depending on the operation requirements, but by convention normally operates at 70  $eV$ . It is found that on average only one ion is produced for every 1000 molecules entering the source under the usual spectrometer conditions, at 70  $eV$ .

Some important ion sources are briefly described in the proceeding paragraphs:

In *chemical ionization* (CI) source, the analyte is ionized by reaction with a set of reagent ions. These reagent ions are formed from the reagent gas by a combination of electron ionization and ion-molecule reactions. The proportion of compound to reactant gas is usually of the order of 1 to 1000, so the electron ionization of the analyte does not occur. One of the most popular reagent gases is methane. Isobutane and ammonia have also been used as reagent gases. In a *thermospray* (TSP) source, a solution containing a

salt and the sample are quickly heated in a steel capillary tube that is heated to a high temperature. The solution then passes through a vacuum chamber as a supersonic beam. As a result a fine droplet spray containing ions and solvent and sample molecules occurs. The ions in the solution are extracted and accelerated towards the mass analyzer.

*Electrospray* (ESP) uses a strong electric field, applied to a liquid with a weak flux (normally 1-10  $\mu l/min$ ) passing through a capillary tube, under atmospheric pressure. An electric field of the order of  $10^6 V/m$  is generated by applying a potential difference of 3-6 *kV* between the capillary and the counter electrode separated by 0.3-2 *cm*. This field induces a charge accumulation at the liquid surface located at the end of the capillary that will break to form highly charged droplets. These droplets undergo a cascade of ruptures, yielding smaller and smaller droplets. When the electric field on their surface becomes large enough, desorption of ions from the surface occurs.

In *spark* sources, electric discharges are used to desorb and ionize the analytes from solid samples. The source consists of a vacuum chamber in which two electrodes are mounted. A pulsed 1 *MHz* rf voltage of several kilovolts is applied in short pulses across a small gap between these electrodes to produce the electric discharge. One of the electrodes is the sample, if the sample is a nonmetal, it can be mixed with graphite and placed in a cup-shaped electrode. The ionization of the atomized sample atoms occurs in the plasma (spark).

In *plasma desorption* (PD), the sample deposited on a small-aluminized nylon foil is exposed in the source to fission fragments of  $^{252}\text{Cf}$  having energy of several *MeV*. The shock waves resulting from the bombardment of a few thousand fragments per second induce the desorption of neutrals and ions.

### 2.4.2 Mass Analyzers

The ions which are produced in the ion source are now transmitted in to the mass analyzer where they are separated according to their masses (rather  $m/z$  ratio), which must be determined.

Scanning analyzers transmit ions of different masses successively along a time scale. Examples of this type are the magnetic sector instruments and quadrupole instruments. Although mass analyzers are generally scanning devices, some allow simultaneous transmission of all ions as in the dispersive magnetic analyzers, the time-of-flight mass analyzer and the ion trap or the ion cyclotron resonance instruments. In tandem mass spectrometry (MS/MS), systems use several analyzers in sequence.

The three important characteristics of an analyzer are the upper mass limit, the transmission and the resolution. The mass limit determines the highest value of the  $m/z$  ratio that can be measured. The transmission is the ratio between the number of ions reaching the detector and the number of the ions produced in the source. The resolving power is the ability to yield distinct signals for two ions with a small mass difference.

The quadrupolar analyzer uses the stability of the (ion) trajectories in oscillating electric fields to separate ions according to their  $m/z$  ratio. This analyzer has four perfectly parallel pole or rods or, ideally, hyperbolic section. Mass sorting depends on ion motion resulting from simultaneously applied constant (dc) and radio frequency (rf) electric fields. Mass scanning is accomplished by systematically changing the field strengths, thereby changing the  $m/z$  value that is transmitted through the analyzer.

Some main mass analyzers are briefly described in the following paragraph:

The *quadrupole ion trap* or quistor operates on a principle similar to a quadrupole mass analyzer. It is made up of a circular electrode, with two ellipsoid caps on the top

and the bottom. The overlapping of a direct potential with an alternative one gives a kind of ‘three-dimensional quadrupole’ in which the ions of all masses are trapped on a three-dimensional trajectory, i.e. the space bounded by the electrodes. The mass scanning is done by varying the applied r.f. voltages to eject the trapped ions sequentially of increasing  $m/z$  ratio. In *time-of-flight* (TOF) analyzer, ions that are expelled from the source are accelerated by potential  $V_s$  and made to fly a distance  $d$  before reaching the detector. Mass-to-charge ( $m/z$ ) ratios are determined by measuring the time that ions take to move through a field-free region between the source and the detector. *Magnetic and electromagnetic* analyzers use the action of the magnetic fields on the motion of the ions to sort the masses. The masses are filtered according to  $m/q = r^2 B^2 / 2V_s$ .

### 2.4.3 Detectors

The ion beam after being sorted by the analyzer is detected and transformed into a usable signal by a detector. The detectors can be put into two categories: the Faraday cage or cup, allows a direct measurement of the charges that reach the detector, and an electron multiplier detectors and array detectors that increase the intensity of the signal. In *Faraday detector* the ion give up their charge on the inside of the cup. The discharge current is then amplified and measured. *Electron multipliers* use a plate (conversion dynode), which causes secondary emissions when positive or negative ions reach it. These secondary particles are accelerated into the continuous-dynode electron multiplier dislodging electrons as they collide with its curving inner walls. This cascade of electrons produced results in a measurable current at the end of the multiplier.

## 2.5 The SRS Residual Gas Analyzer

Stanford Research System's (SRS) Residual Gas Analyzer (RGA) 300 was used to conduct studies. The *SRS RGA* is a mass spectrometer consisting of a quadrupole probe, and an electronics control unit (ECU) which mounts directly on the probe's flange, and contains all the electronics necessary to operate the instrument (*see* Figure 2-4). The probe has the quadrupole mass analyzer that is mounted directly onto a 6.985 cm (2 3/4") CF port of the vacuum chamber. The total probe equipment consists of three parts: the ionizer (electron impact), the quadrupole mass analyzer and the ion detector. All these parts reside in the vacuum space formed by a stainless steel tube (CF cover nipple) covering the probe assembly with the exception of the ionizer. The *ECU* connects directly to the probes' feedthru-flange and also to the computer through a standard RS232 communications port. The *SRS RGA 300* has mass range from 1 to 300 *amu* and operating pressures are from UHV to  $10^{-4}$  Torr.

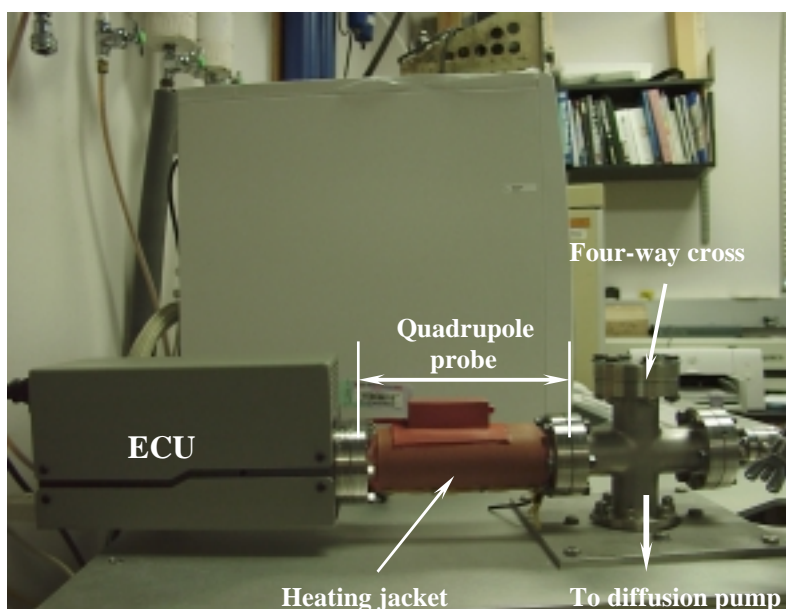


Figure 2-4. *SRS* Mass spectrometer.

### 2.5.1 Ionizer

The *SRS RGA* ionizer is of wire mesh construction with cylindrical symmetry and mounted co-axially with the mass filter assembly. The main parts of the ionizer are the repeller, the anode grid, the filament, and the focus plate (*see* Figure 2-5).

The filament is an oxidation-resistant thoria coated iridium wire. It operates at a negative potential relative to ground and resistively heated with an electric current. The emitted electrons are accelerated towards the anode grid, which is positively charged with reference to the filament and the ground. Because of the design of the anode grid cage, most electrons do not strike the anode immediately, but pass through the cage where they

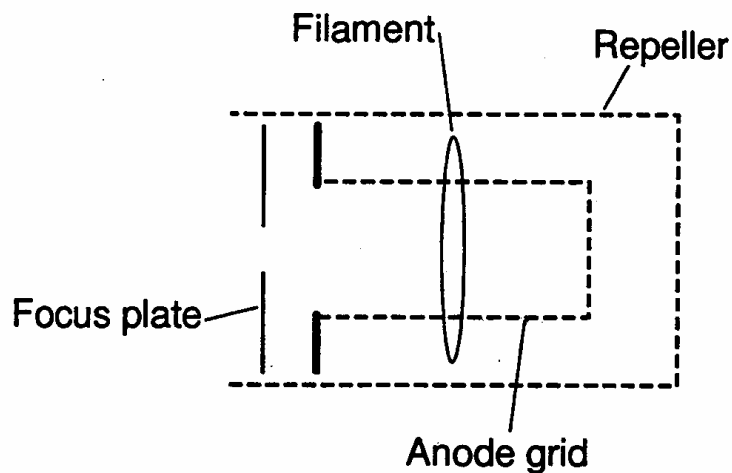


Figure 2-5. Ionizer Schematic. Reproduced from Ref. 4.

create ions. Ions once formed stay within the anode grid structure, and ion distribution is more localized along the axis. The ions formed within the anode grid volume are extracted from the ionizer by the electric field produced by the difference in voltage bias between the anode grid and the focus plate. The focus plate is kept at a negative potential relative to ground and its function is to draw the ions out of the anode cage and focus

them into the analyzer section. The repeller is biased negative relative to the filament and prevents the loss of electrons from the ion source.

### 2.5.2 Quadrupole Mass Filter:

The analyzer is built of four stainless steel (type 304) cylindrical rods (11.43 cm long, 0.635 cm diameter) accurately held in place by a set of two high-purity alumina insulators. The electrodynamic quadrupole field is produced by a combination of *dc* and *rf* voltages.

During operation, a 2-*d* (*x-y*) quadrupole field is established between the four cylindrical electrodes with the two opposite rods connected together electrically. Ions enter the filter along the *z*-axis and start oscillating in the *x*- and *y*- directions.

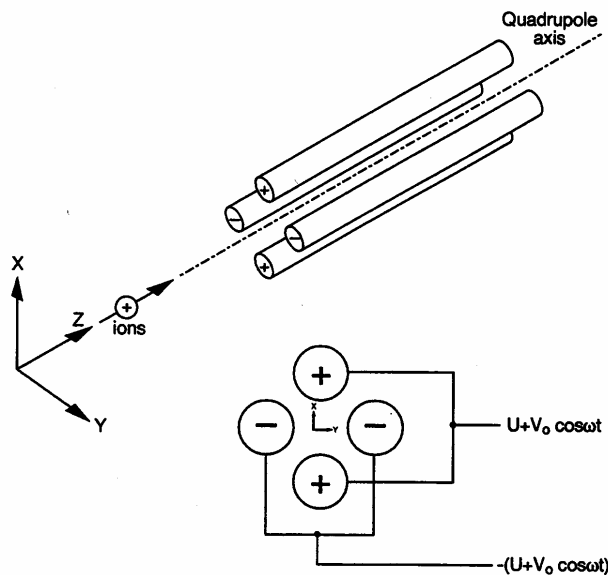


Figure 2-6. Quadrupole rod connections. Reproduced from Ref. 4.

The general principle of operation of the analyzer can be visualized qualitatively as: one rod pair (*xz* plane) is connected to a positive *dc* voltage with a superimposed sinusoidal *rf* voltage. The other rod pair (*yz* plane) is connected to a negative *dc* voltage

upon which a sinusoidal *rf* voltage is superimposed,  $180^\circ$  out of phase with the *rf* voltage of the first set of rods (*see* Figure 2-6). The potentials are given by the expression:

$$\begin{aligned}\phi_0 &= (U + V \cos \omega t) \\ \phi_0 &= -(U + V \cos \omega t)\end{aligned}$$

In this equation,  $U$  is the magnitude of the *dc* voltage applied to either pair of rods,  $V$  is the amplitude of the *rf* voltage applied to either set of rods, and  $\omega$  is the angular frequency ( $=2\pi f$ ) of the *rf*. The ions accelerated along the  $z$ -axis are submitted to the following forces:

$$\begin{aligned}F_x &= m \frac{d^2 x}{dt^2} = -ze \frac{\partial \phi}{\partial x} \\ F_y &= m \frac{d^2 y}{dt^2} = -ze \frac{\partial \phi}{\partial y}\end{aligned}$$

where  $\phi$  is a function of  $\phi_0$ :

$$\phi_{(x,y)} = \phi_0(x^2 - y^2)/r_0^2 = (x^2 - y^2)(U + V \cos \omega t)/r_0^2$$

where  $r_0$  is the radius of the circle inscribed by the quadrupole rods. Derivatizing and rearranging the terms leads to following equations of motion:

$$\begin{aligned}\frac{d^2 x}{dt^2} + \frac{2ze}{mr_0^2}(U + V \cos \omega t) &= 0 \\ \frac{d^2 y}{dt^2} - \frac{2ze}{mr_0^2}(U + V \cos \omega t) &= 0\end{aligned}$$

For  $x, y \neq r_0$ , the trajectory of the ion will be stable. That means the ion never hits the rods. The above equations are in the form of the Mathieu equation:

$$\frac{d^2u}{d\xi^2} + (a_u - 2q_u \cos 2\xi)u = 0$$

comparing the preceding equations with this one, we have:

$$\xi = \frac{\omega t}{2}, \quad a_u = a_x = -a_y = \frac{8zeU}{m\omega^2 r_0^2}$$

and,  $q_u = q_x = -q_y = \frac{4zeV}{m\omega^2 r_0^2}$

from the above relations we can deduce:

$$U = a_u \left( \frac{m}{z} \right) \left( \frac{\omega^2 r_0^2}{8e} \right) \quad \text{and} \quad V = q_u \left( \frac{m}{z} \right) \left( \frac{\omega^2 r_0^2}{4e} \right)$$

The last two terms of both the  $U$  and  $V$  equations are constant for a given quadrupole instrument as they operate at constant  $\omega (= 2\pi f)$ .

### 2.5.3 Ion Detector

Positive ions that successfully pass through the quadrupole are then focussed towards the detector by an exit aperture held at ground potential. The detector components are shown in the Figure 2-7.

The Faraday Cup (FC) detector, is a 304 stainless steel bucket, measures the incident ion current directly. It is shielded from the intense RF and DC fields of the quadrupole by the grounded exit plate. A cylindrical tube (FC shield) encloses the FC, protecting it from the strong electrodynamic potentials of the adjacent rods and from

collecting ions originated other than the ionizer. Positive ions enter the grounded detector and give up their charge on the wall. The electrons given up in this process establish an electrical current that has the same intensity as the incoming ion current. The nominal sensitivity of the RGA is in the order of  $10^{-4}$  amps/torr. Minimum-detectable partial pressures as low as  $5 \cdot 10^{-11}$  Torr are possible with FC.

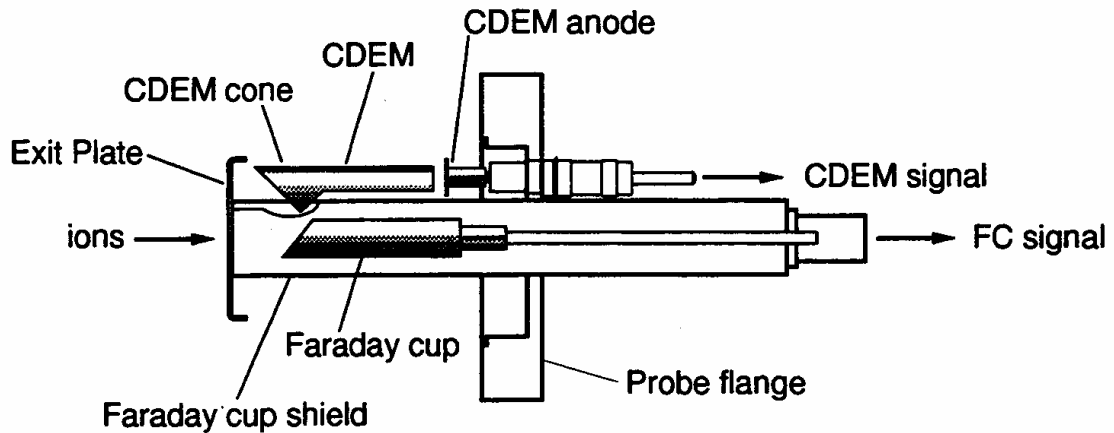


Figure 2-7. Ion Detector Components. Reproduced from Ref. 4.

#### 2.5.4 Modes of Operation of SRS RGA

There are four basic modes of operation of the mass spectrometer: analog scanning, histogram scanning, single mass measurement and total pressure measurement. In analog scanning the mass spectrometer is stepped at fixed mass increments through a pre-specified mass range. The ion current is measured after each mass increment step and transferred to the host computer over RS232. In leak detection measurement mode (single mass measurement), the RGA can measure individual peak heights at any integer mass within its mass range. This mode of operation is used to generate data for leak testing measurements, and to track changes in the concentrations of several different components of a mixture as a function of time.

## 2.6 Vacuum System

The SRS mass spectrometer operates at pressure ranging from  $10^{-4}$  Torr to UHV. The mass spectrometer was mounted onto a standard 6.985 cm (2¾") CF port of a 4-way cross connector. The diffusion pump is connected to one side of the 4-way cross. The vacuum chamber is comprised of the probe volume and the 4-way cross volume. The required vacuum environment in this chamber was achieved using a diffusion pump and a rotary pump connected in series. A second rotary pump was connected to the sampling port to suck in the sample gas and also pumps away negative ions and gases from the vacuum chamber (*see* Figure 2-8).

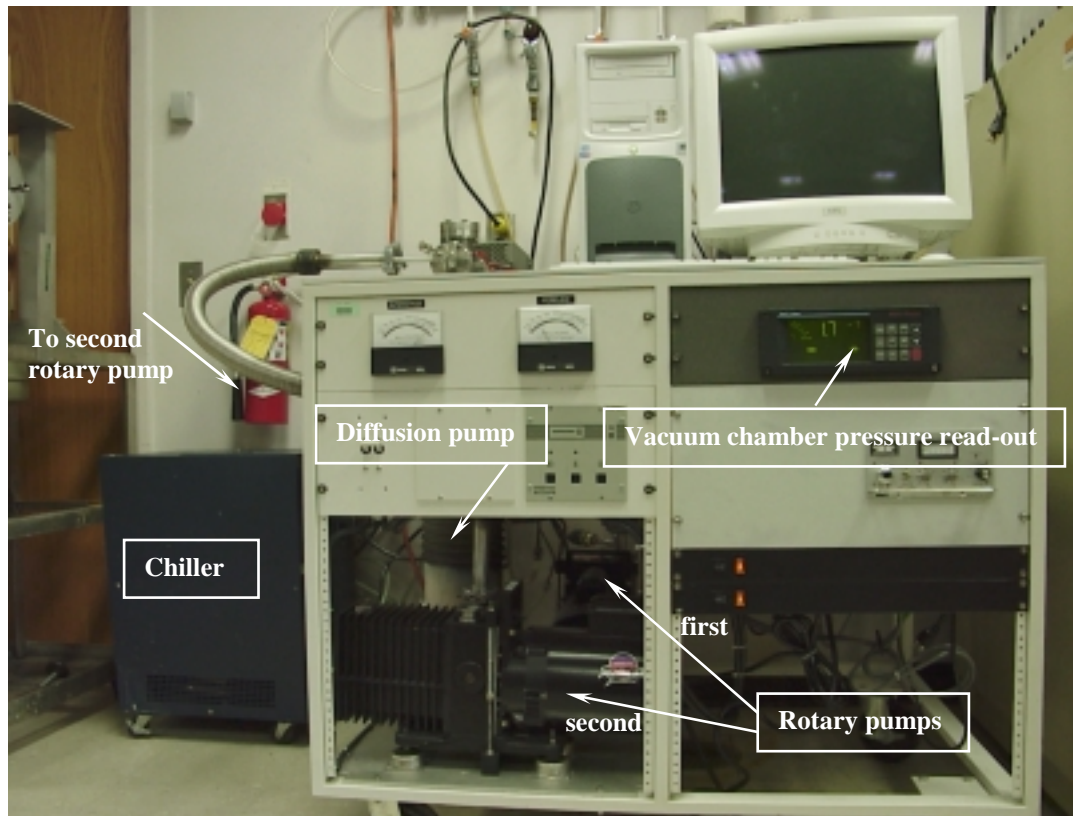


Figure 2-8. Vacuum pumping system.

## CHAPTER 3 RESULTS AND SUMMARY

### 3.1 Introduction

In this study, preliminary work has been done to evaluate the application of quadrupole mass spectrometry (SRS RGA 300) to two distinct situations: gas leak detection and ionization of fuels. For the leak detection studies the focus was to determine the trend of concentration gradients for a gas leak until the time it takes to reach a steady state. In the ionization studies effort was made to determine the intensity of ion production as a function of ionization potential, i.e. for various degrees of ionization.

### 3.2 Data Acquisition and Calibration

The first step in data acquisition (scanning) requires establishing a connection between the RGA program and the head. The data is carried out over the RS232 cable to the computer. Then a desired scanning mode is selected and the filament is turned on. Next the desired scan parameters and trigger rate are selected to start the scan.

The SRS mass spectrometer was calibrated at the factory and it was checked for the accuracy of mass scale calibration prior to testing. Towards this effort, few analog scans for a mixture of argon and helium and air were taken and checked for the peak positions of Ar, He, N<sub>2</sub>, O<sub>2</sub>, CO<sub>2</sub>, and H<sub>2</sub>O. The peaks were seen at the desired positions on the mass scale (*see* Figure 3-1).

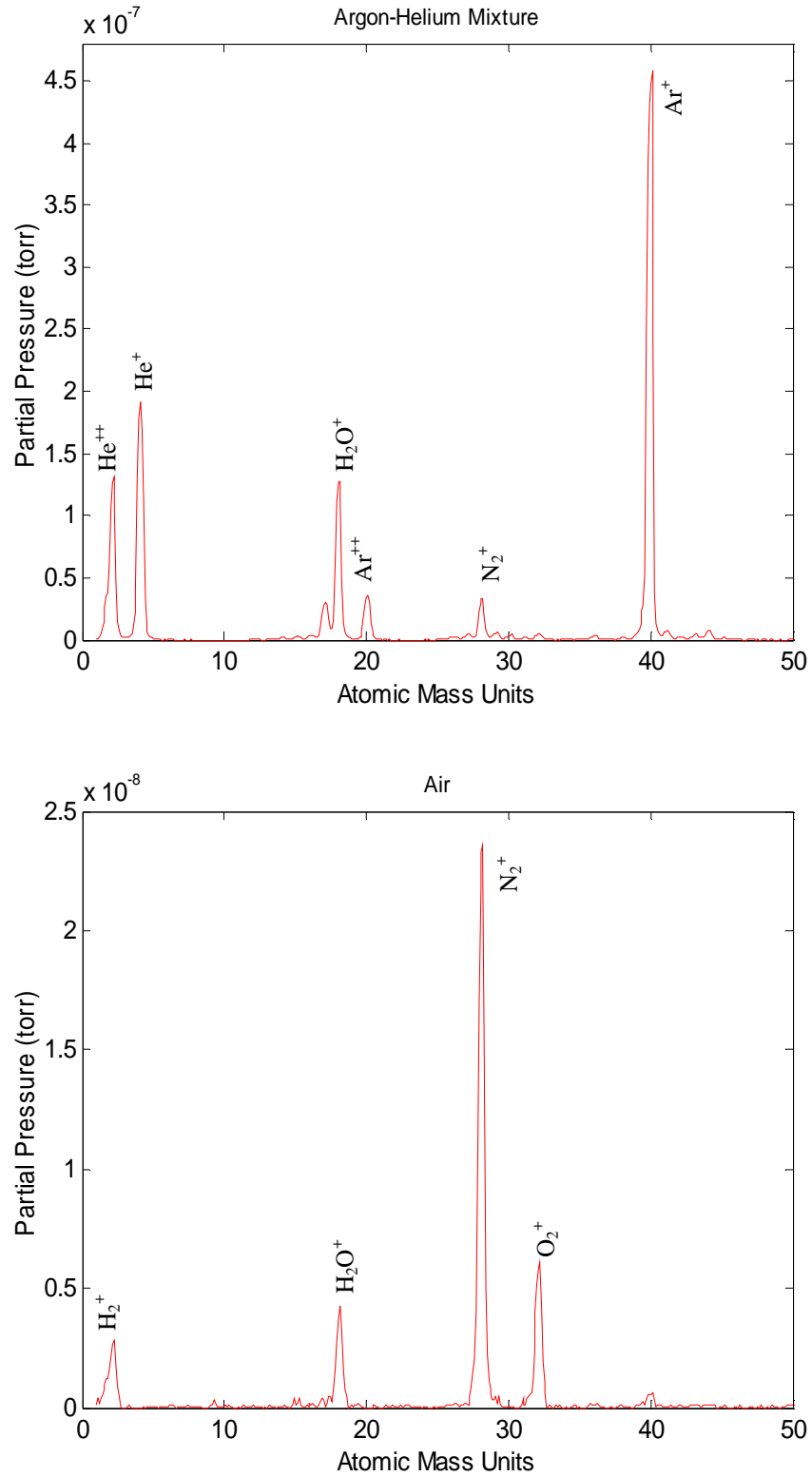


Figure 3-1. Analog scans- mass scale calibration.

### 3.2 Leak Detection Tests

The leak detection tests were carried out using the Leak Test mode available in the RGA Windows program. This mode provides the most effective way to monitor a single gas species.

During the initial runs, a helium ( $amu=4$ ) leak at a pressure of  $P_{He}=241\text{ kPa}$  was initiated through a  $1.6\text{ mm}$  tygon tube at a predetermined location inside the aft compartment model. The air purge rate into the model was  $0.012\text{ SCMS}$ . The sampling to the mass spectrometer was done with a  $1.6\text{ mm}$  tygon tube taken from a predetermined sampling point. The tests were conducted at Scan Speed ( $SS$ ) of 3, i.e. Noise Floor ( $SS-1$ ) of 2 and the mass spectrometer was triggered every  $5\text{ sec}$ . The mass spectrometer did not detect any trace of helium even after 1 hr and the run was terminated. Various runs were repeated at similar conditions and for different sample and leak ports without He detection.

Therefore calibration test have been initiated into a smaller volume. A helium leak at  $P_{He}=14\text{ kPa}$  was initiated into a small box with a volume of  $1500\text{ ml}$ . The runs were conducted at  $SS=3$  and triggering of  $4\text{ sec}$  and for two different lengths of separation of  $L=1.3\text{ cm}$  and  $L=2.5\text{ cm}$  between the leak and the sample point. Helium detection was observed for this set of runs. Figures. 3-2 and 3-3 shows the curves of He concentration for the four leak test runs as Mean Normalized Pressure vs. Time, each taken at  $L=1.3$  and  $L=2.5\text{ cm}$  respectively. The steady state detection is achieved within  $5.25\text{ sec}$  for  $L=1.3\text{ cm}$  and  $5.5\text{ sec}$  for  $L=2.5\text{ cm}$ .

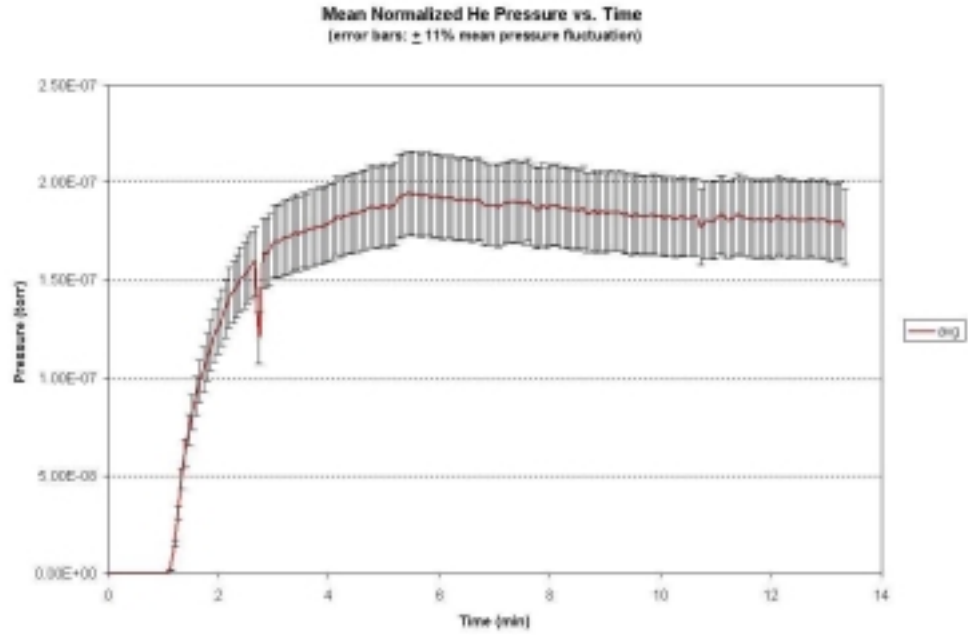


Figure 3-2. Helium leak detection concentration curve for  $L=1.3$  cm

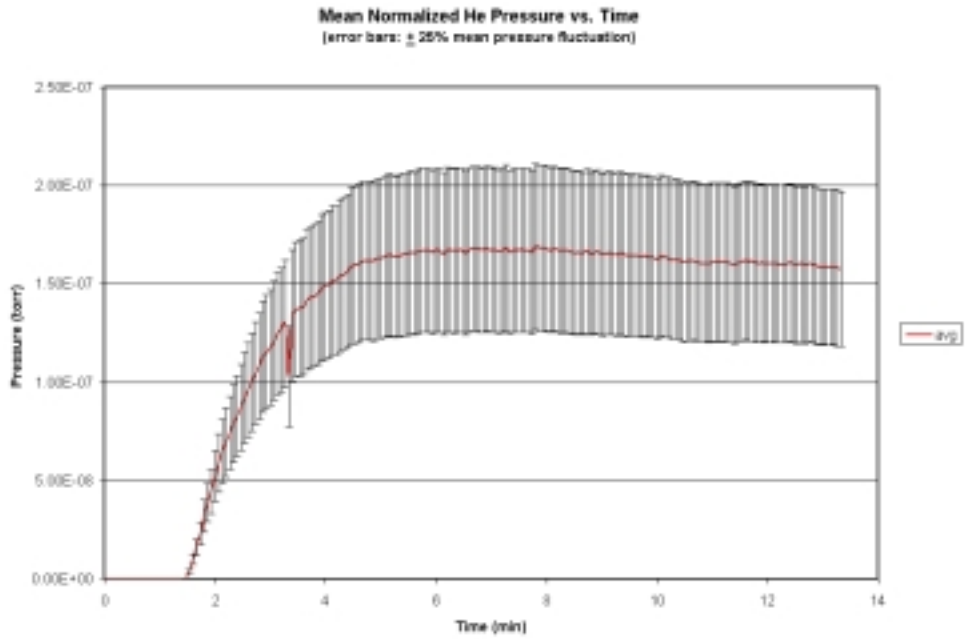


Figure 3-3. Helium leak detection concentration curve for  $L=2.5$  cm.

### 3.3 Ionization Tests

For the ionization tests ‘Analog mode’ was used to take the scans. In Analog mode the RGA Head scans from the start to the stop mass using the points per amu variable specified in the Mass Spec Parameters dialog box. The  $x$ -axis represents the mass range chosen and the  $y$ -axis represents the partial pressures of individual species in the gaseous mixture. The mass spectrometer head and scan parameters used for the scans were the default values. In the SRS mass spectrometer a scan cannot be taken without switching the filament on. This is an inherent limitation with regards to the operation of this mass spectrometer. The ionization tube is an external ion-generating source. The degree of ionization obtained within the ionization tube can be truly quantified when the internal ionization due to the mass spectrometer’s ionizer is completely eliminated. Therefore to accomplish this the filament must be removed from the ionizer assembly.

Tests were conducted to study the intensity of ionization/fragmentation of butane ( $C_4H_{10}$ ) gas. Butane was introduced into the mass spectrometer bypassing the ionization tube. The effects of internal ionization on butane were studied at 25, 40 and 70  $eV$  ionization potential. The scans shown in Figure 3-4 indicate increased intensity and fragmentation of butane into smaller species with increasing ionization potential. The major fragmentation species observed were  $CH_3^+$ ,  $C_2H_3^+$ ,  $C_2H_4^+$ ,  $C_2H_5^+$ ,  $C_3H_5^+$ ,  $C_3H_6^+$ , and  $C_3H_7^+$ . The Figure 3-5 shows a plot of fragmentation species pressure normalized by parent ion pressure ( $C_4H_{10}^+$ ) versus atomic mass units. From this plot it can be seen that the methyl radical,  $CH_3^+$ , is not formed at 25  $eV$  ionization potential. Further tests were conducted on argon gas to compare the intensity of external ionization obtained in the ionization tube to that obtained within the mass spectrometer ionizer. The results show

that the ionization obtained within the ionization was a miniscule when compared to that produced within the mass spectrometer.

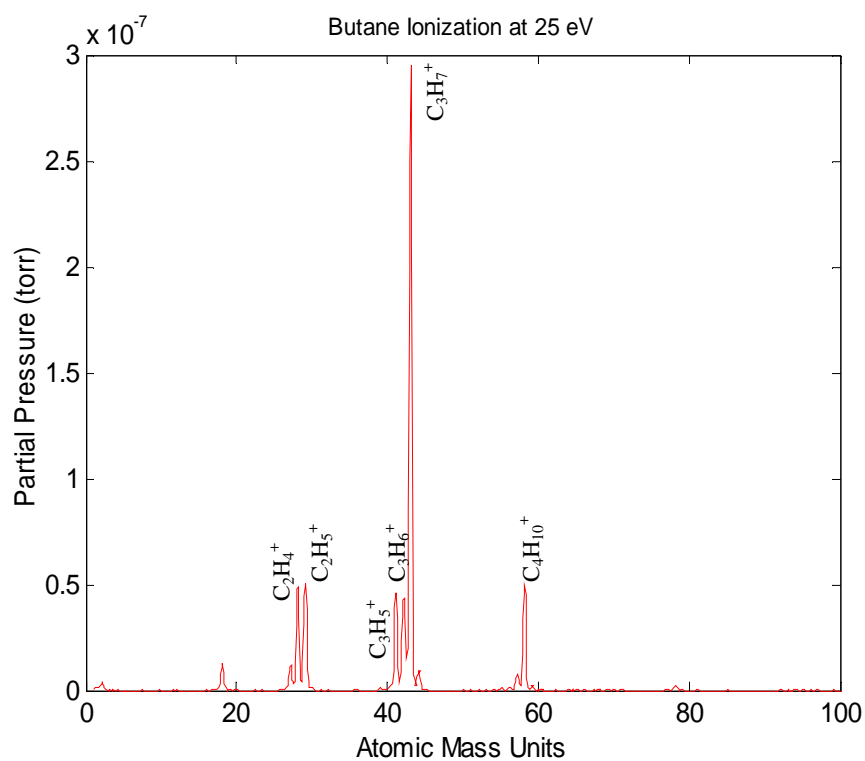


Figure 3-4. Butane ( $C_4H_{10}$ ) ionization.

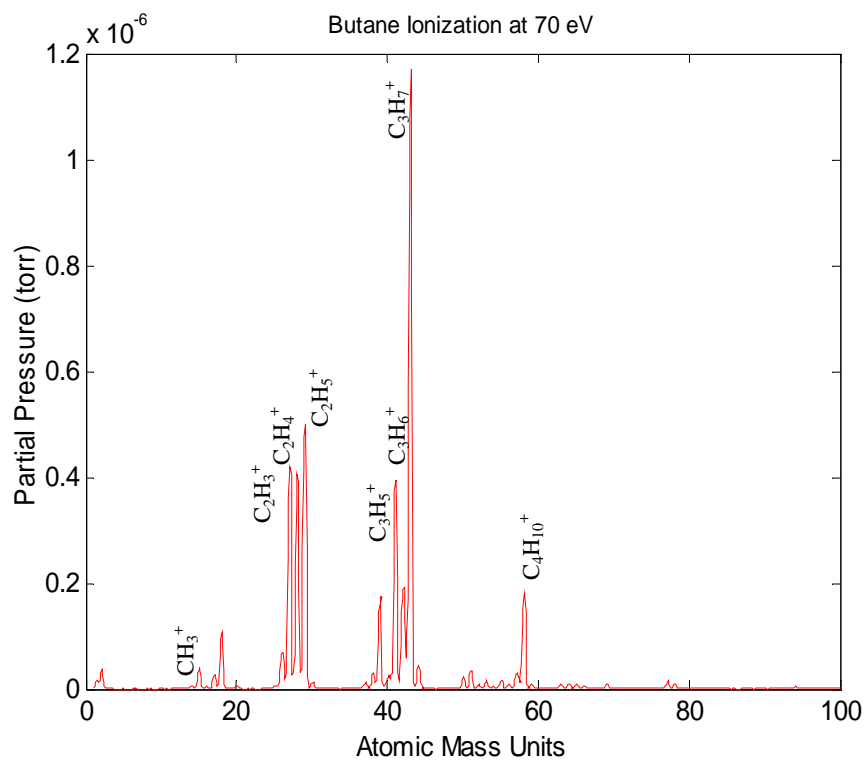
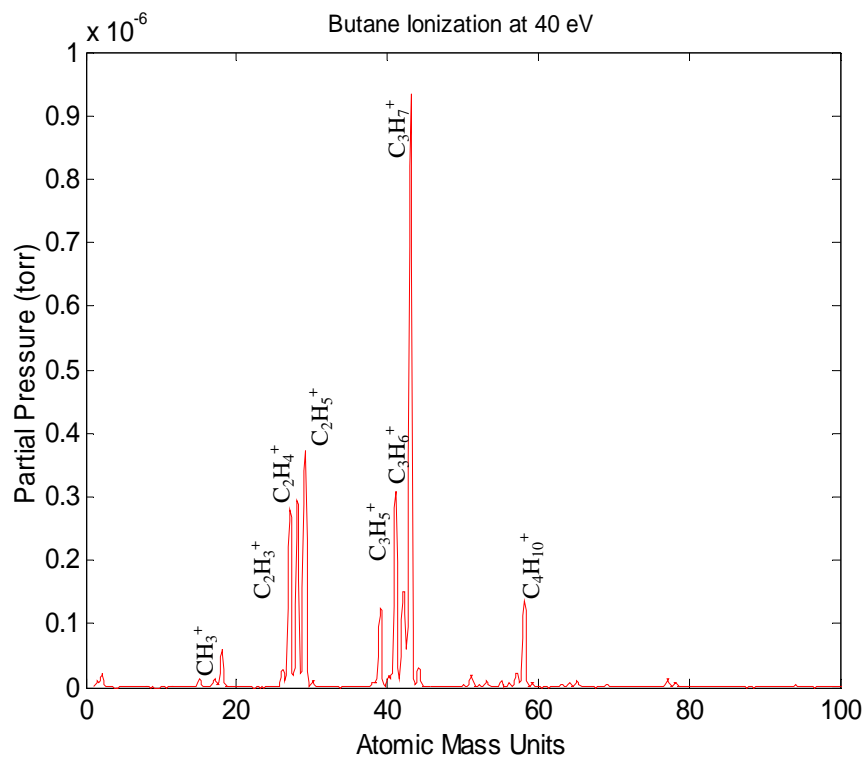


Figure 3-4 (contd.). Butane ( $\text{C}_4\text{H}_{10}$ ) ionization.

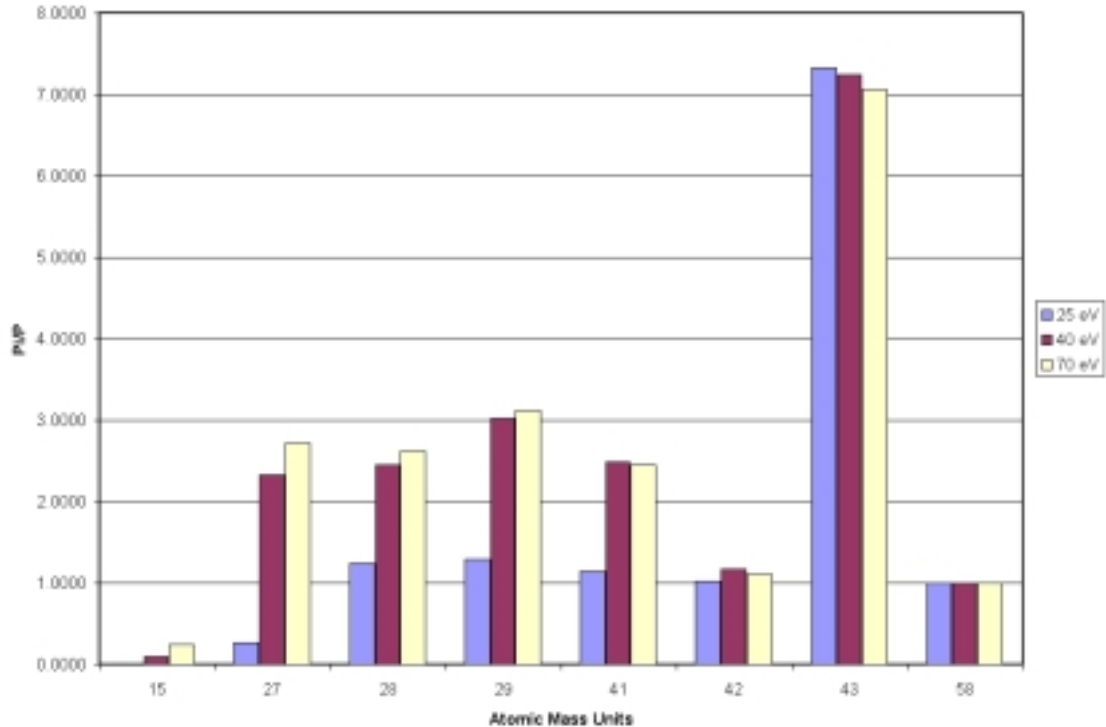


Figure 3-5. Normalized fragmentation species pressure.

### 3.5 Summary

The present study evaluated the mass spectrometry system developed for two distinct applications of leak detection and ionization of hydrocarbon gases. The results are summarized in the proceeding paragraphs:

The mass spectrometry system was not able to detect any trace of He leak in the aft compartment model for both purge on and off modes. Some of the possible reasons for this problem are:

- (1) The amount of leak initiated into the aft compartment model was low at the conditions tested and the detection results were, therefore, inconsistent.
- (2) In the case of ionization tube, the true amount of ionization produced in the tube might be higher than that produced internally in the ionizer. However the study has shown that the internal ionization is more than that of the external ionization. One of the reason for this defect may be the externally produced ions might not be reaching the ion detector due to kinetic energy losses and

divergence. This problem may be overcome by accelerating the ions into the mass spectrometer using a set of electrostatic lenses with increasing negative potential applied to the successive lens.

APPENDIX A  
AFT COMPARTMENT MODEL

This appendix gives the drawings used to construct the hull of the aft compartment model. The compartment model is scaled to 1:4, and of plexiglass outer construction. All the dimensions in the drawings are in meter.

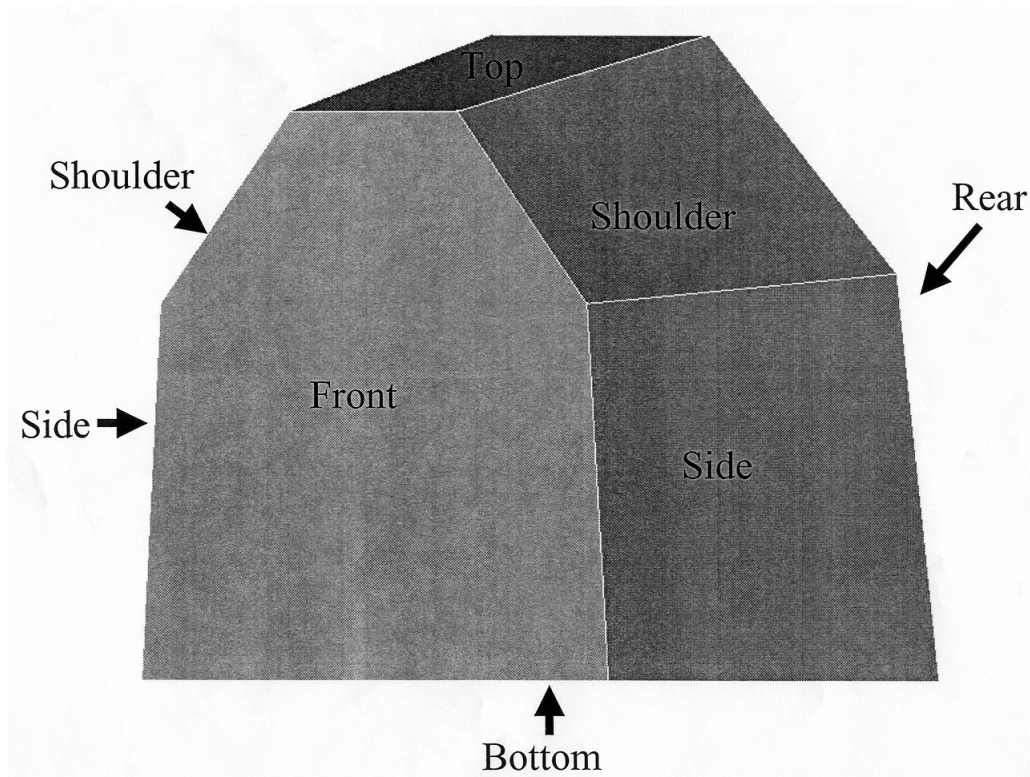


Figure A-1. Hull.

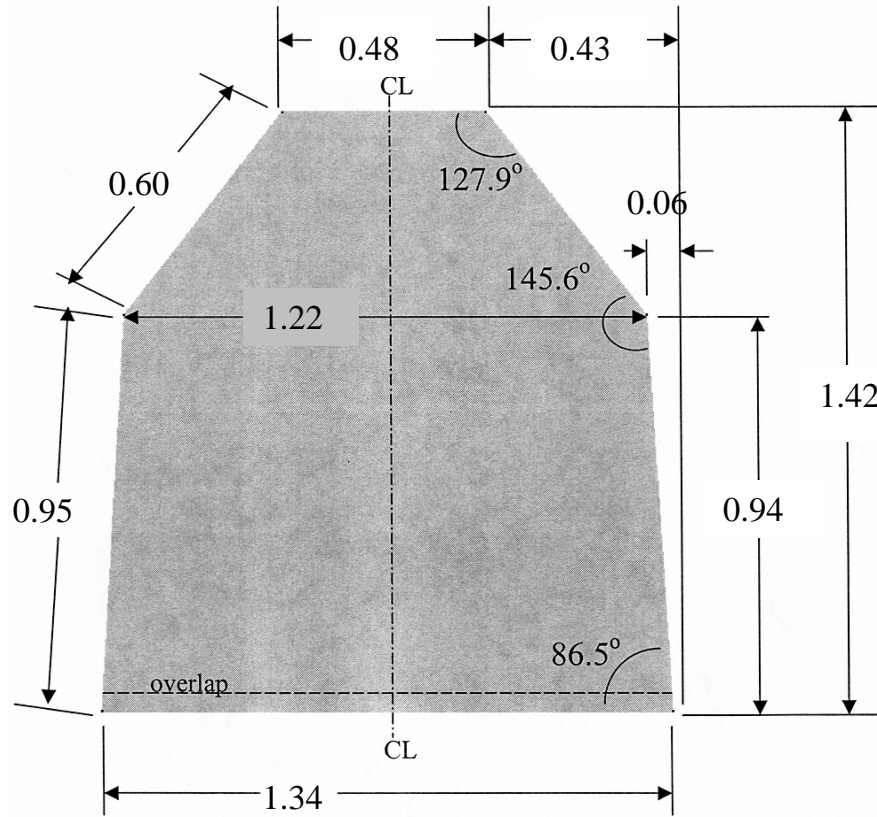


Figure A-2. Hull-front piece.

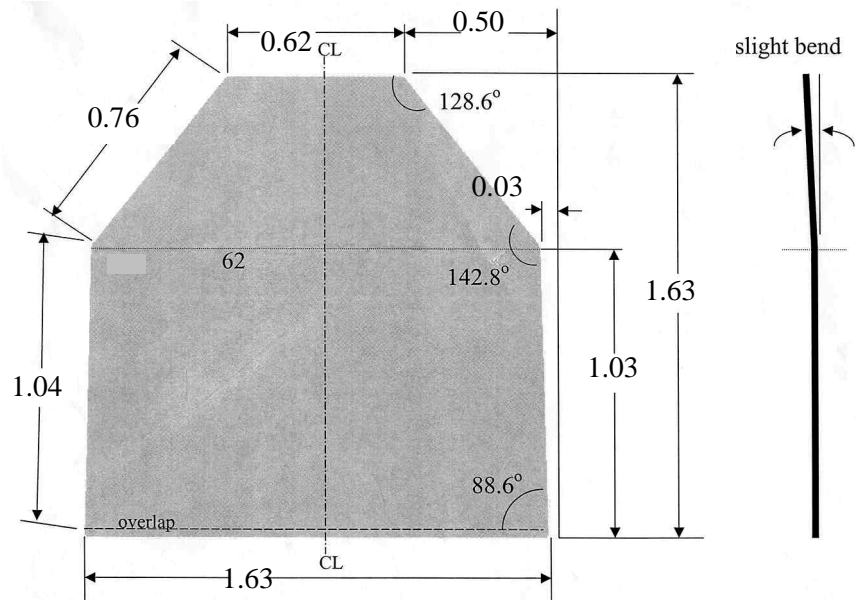


Figure A-3. Hull- rear piece.

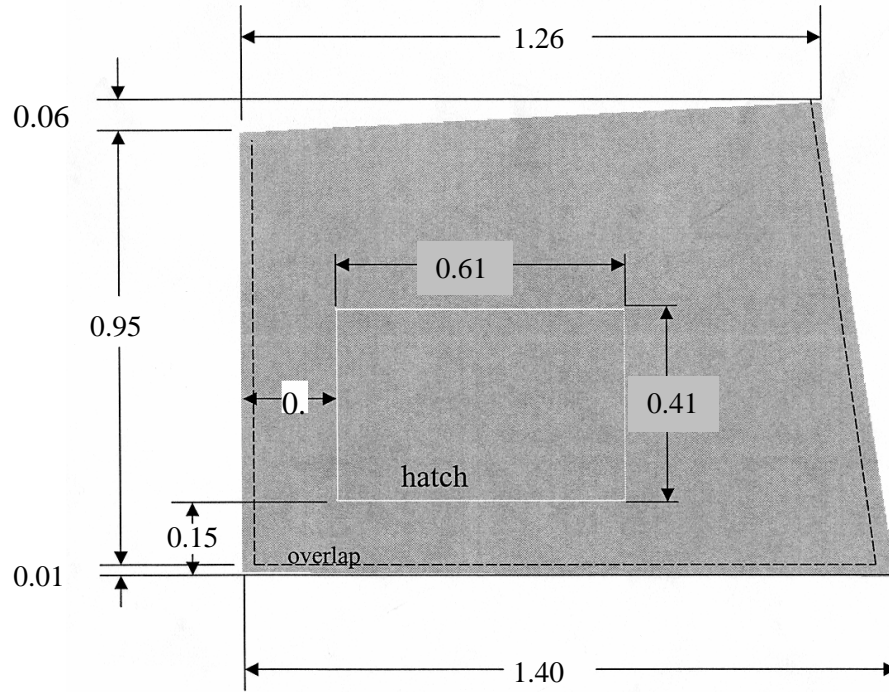


Figure A-4. Hull- side piece.

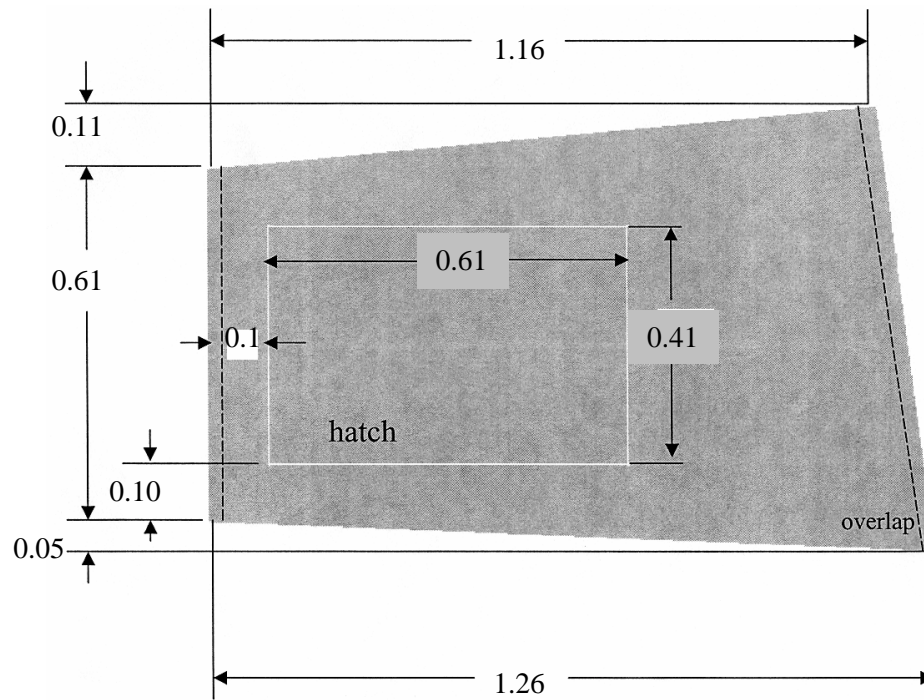


Figure A-5. Hull- shoulder piece.

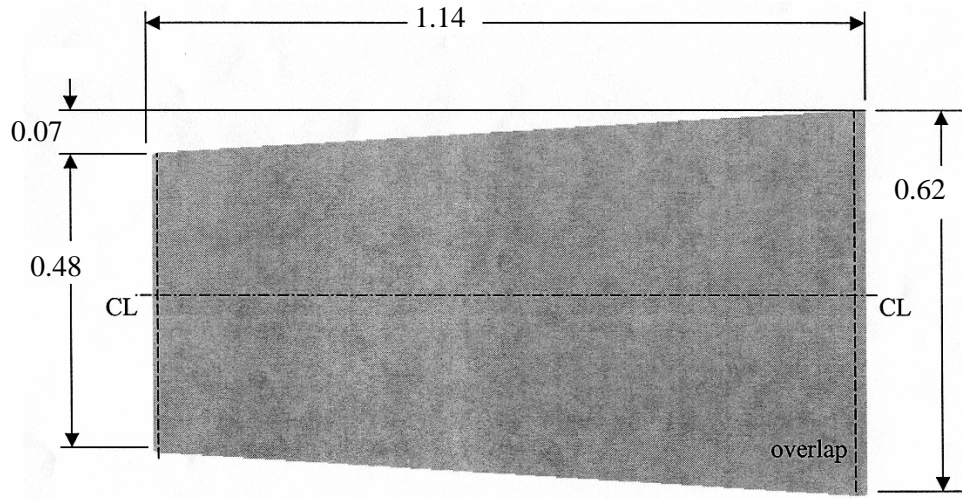


Figure A-6. Hull- top piece.

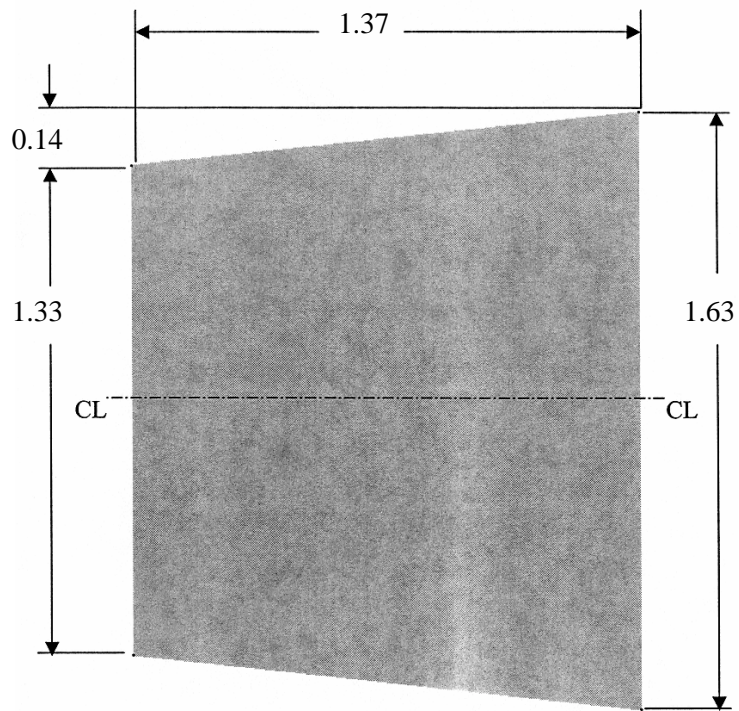


Figure A-7. Hull- bottom piece.

APPENDIX B  
STANFORD RESEARCH SYSTEMS RESIDUAL GAS ANALYZER 300

This appendix gives some of the specifications and figures (internal components) of the SRS RGA 300 mass spectrometer and a typical electrostatic ion lens assembly used to accelerate ions in to the mass spectrometer.

B.1 SRS Mass Spectrometer

B.1.1 Specifications

*Mass Range:* 1 to 300 amu

*Mass Filter Type:* Quadrupole

*Detector Type:* Faraday Cup (FC)

*Resolution:* Better than 0.5 amu @ 10% peak height

*Sensitivity (A/Torr):*  $2 \cdot 10^{-4}$  (FC)

*Minimum Detectable Partial Pressure:*  $5 \cdot 10^{-11}$  Torr

*Operating Pressure Range:*  $10^{-4}$  Torr to UHV

*Design:* Open source, cylindrical symmetry

*Operation:* Electron ionization

*Material:* Stainless steel, type 304

*Filament:* Thoriated iridium

*Electron Energy:* 25 to 105 V

*Ion Energy:* 8 or 12 V

*Focus Voltage:* 0 to 150 V

*Electron Emission Current:* 0 to 3.5 mA

*Computer Interface:* RS-232C, 28800 Baud

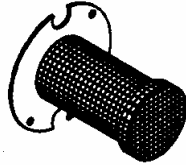
*Software:* Windows OS based application (RGA Windows)

B.1.2 Internal Components

**Focus Plate**



**Anode Grid**



**Filament**



**Repeller**

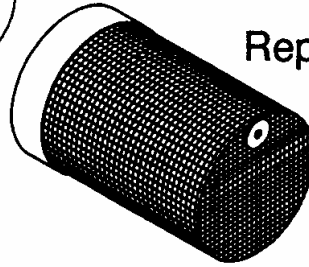


Figure B-1. Ionizer Components.

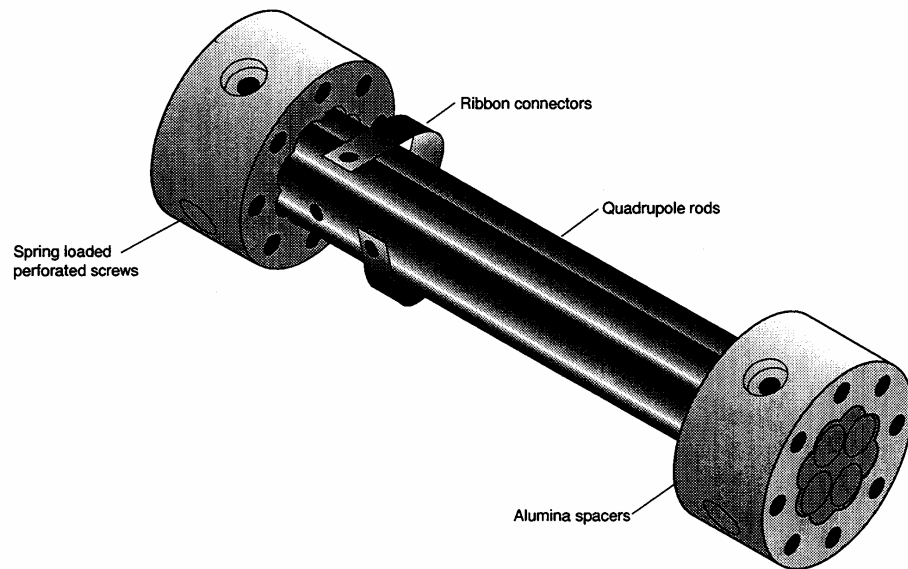


Figure B-2. Quadrupole Mass Filter Components.

## B.2 Electrostatic Ion Lens System

The high-speed hydrocarbon ions produced in the ionization tube tend to have decreasing kinetic energy and increasing divergence as they move along the length of the vacuum system until they reach the quadrupole mass analyzer. These problems can be overcome with the help of an ion lens system.

An electrostatic ion lens system is placed between the ion source (ionization tube) and the quadrupole mass analyzer and is enclosed in the vacuum chamber. The function of an electrostatic ion lens system is to collect positive ions from the supersonic jet of sampled gas while neutral particles are pumped away. The ions are then focussed and transmitted to the mass analyzer. A typical ion lens system is shown in Figure B.3, which consists of a set of coaxial, sequential cylinders, each biased at a particular *dc* voltage. The ion system is tuned to a particular set of *dc* voltages such that maximum ion signals are obtained.

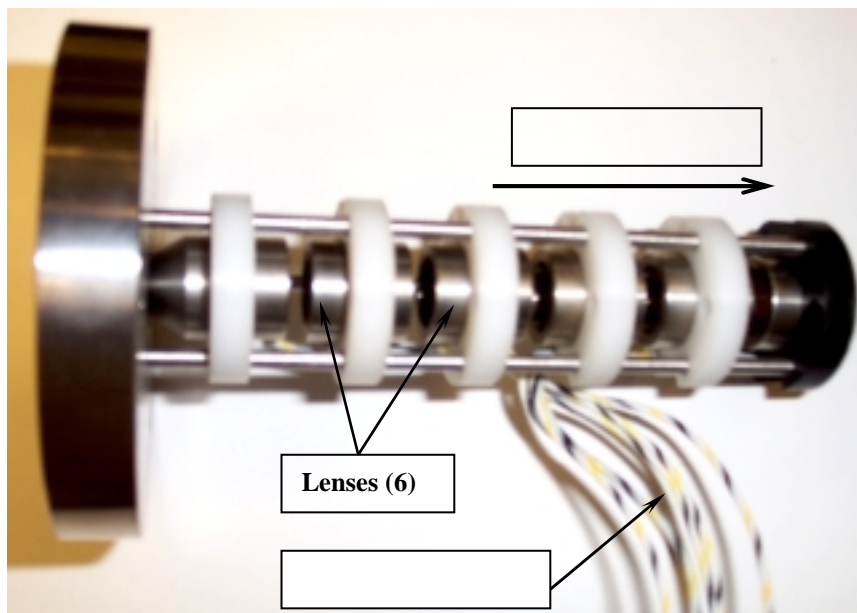


Figure B-3. Electrostatic ion lens system.

A schematic diagram of ICP, ion sampling interface and vacuum system is shown in Figure B.4. The components shown in the schematic are: (1) analyte introduction, (2) ICP torch and load coil, (3) shielding box, (4) skimmer with plasma plume shown streaming through the central hole, (5) sampler cone with extraction orifice, (6) electrostatic lens assembly, (7) quadrupole mass analyzer, (8) electron multiplier, (9) pumping port to first pumping stage, and (10) pumping port to second pumping stage.

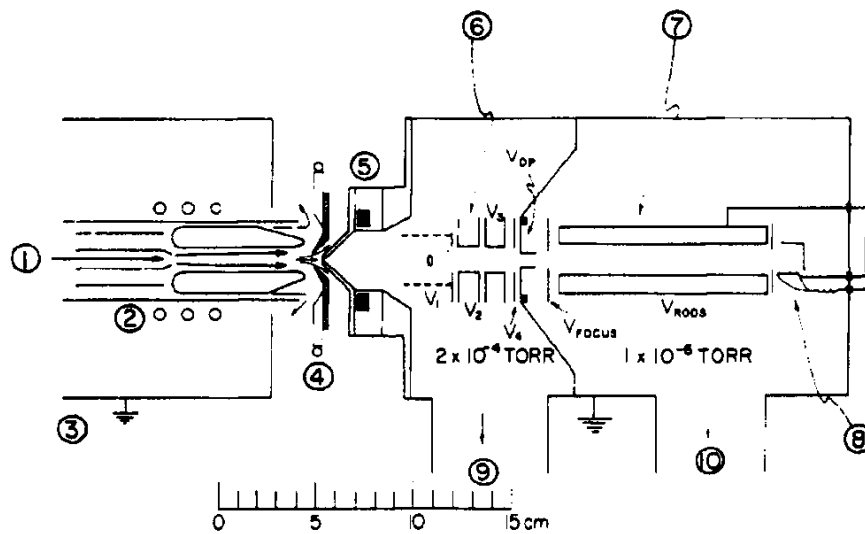


Figure B-4. ICP, ion sampling interface, and vacuum system. Reproduced from Ref. 21.

The system shown above can be adapted for the SRS mass spectrometer system as shown in the Figure B-5. The vacuum chamber houses an electrostatic ion lens system similar to that shown in Figure B-3. The chamber has 3 ports namely, a pinhole, a pumping port and a port to connect to the 2 3/4" CF flange of the SRS quadrupole probe. The entire ionizer assembly of the SRS mass spectrometer is physically removed for this arrangement except the focus plate.

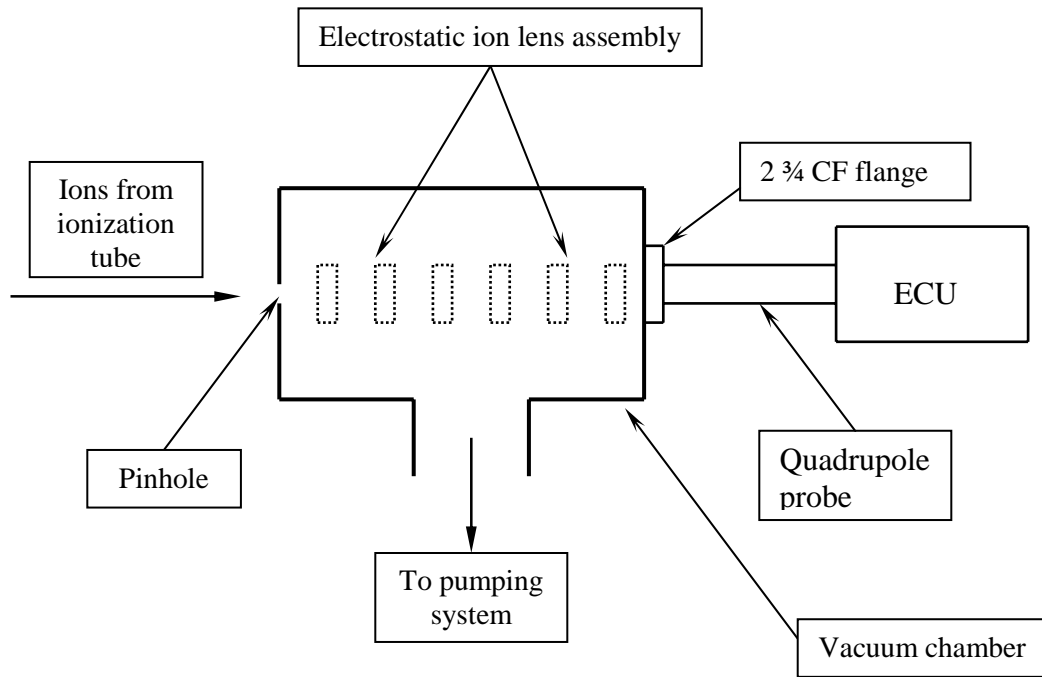


Figure B-5. Schematic of SRS mass spectrometer with the electrostatic ion lens assembly for ionization studies.

## LIST OF REFERENCES

1. T.P. Griffin, G.R. Naylor, W.D. Haskell, C. Curley, R.J. Hritz, G.S. Breznik, C. Mizell, "Hazardous Gas Detection System 2000," NASA Technical Briefs, 2001.
2. NASA KSC WebPages, "Portable Aft Mass Spectrometer (PAMS)," URL: <http://technology.ksc.nasa.gov/WWWaccess/techreports/96report/instf/inst17.html>
3. T.P. Griffin, G.S. Breznik, C.A. Mizell, W.R. Helms, G.R. Naylor, W.D. Haskell, "A Fully-redundant, On-line, Mass-spectrometer System Used to Monitor Cryogenic Fuel Leaks on the Space Shuttle," Trends in Analytical Chemistry, vol. 21, no. 8, pp 488-497, 2002.
4. Stanford Research Systems, Operating Manual and Programming Reference, Models RGA 100, RGA 200, RGA 300 Residual Gas Analyzer.
5. M. Mizukami, G.P. Corpening, R.J. Ray, N. Hass, K.A. Ennix, S.M. Lazaroff, "Linear Aerospike SR-71 Experiment (LASRE): Aerospace Propulsion Hazard Mitigation Systems," NASA/TM, 206561, 1998.
6. N. Hass, M. Mizukami, B.A. Neal, C.St. John, R.J. Beil, T.P. Griffin. "Propellant feed system leak detection-Lessons learned from the Linear Aerospike SR-71 Experiment (LASRE)," NASA/TM, 206590, 1999.
7. H.K. Rivers, J.G. Sikora, S.N. Sankaran, "Detection of Hydrogen Leakage in a Composite Sandwich Structure at Cryogenic Temperature," J. of Spacecraft and Rockets, 39, pp452-459, 2002.
8. A. Chutjian, M.R. Darrach, V. Garkanian, S.P. Jackson, T.D. Molsberry, O.J. Orient, D. Karmon, P.M. Holland, D. Aalami, "A Miniature Quadrupole Mass Spectrometer Array and GC for Space Flight: Astronaut EVA and Cabin-Air Monitoring," Society of Automotive Engineers, Inc., 2000-01-2300.
9. G.W. Hunter, Liang-Yu Chen, P.G. Neudeck, D. Knight, Chung-Chiun Liu, Quing-Hai Wu, Huan-jun Zhou, "Chemical Gas Sensors for Aeronautic and Space Applications," NASA/TM, 107444, 1999.
10. A. Vertes, R. Gijbels, F. Adams, "Diagnostics and Modeling of Plasma Processes in Ion Sources," Mass Spectrometry Reviews, 9, pp71-113, 1990.
11. M.A. Duncan, "Frontiers in the Spectroscopy of Mass-selected Molecular Ions," Int. J. of Mass Spectrometry, 200, pp545-569, 2000.

12. Yu.Ya. Buriko, V.A. Vinogradov, V.F. Goltsev, "Estimation of the Possibility of a Rise in Chemical Activity of Hydrocarbon Fuel Through Injection Free Radicals," Central Institute of Aviation Motors, Moscow, Russia.
13. S. Williams, A.J. Midey, S.T. Arnold, P.M. Bench, A.A. Viggiano, R.A. Morris, L.Q. Maurice, C.D. Carter, "Progress on the Investigation of the Effects of Ionization on Hydrocarbon/Air Combustion Chemistry," AIAA 99-4907, 1999.
14. S.T. Arnold, A.A. Viggiano, R.A. Morris, "Rate Constants and Branching Ratios for the Reactions of Selected Atmospheric Primary Cations with n-Octane and Isooctane (2,2,4-trimethylpentane)," J. Phys. Chem. A, 101, pp9351-9358, 1997.
15. S.T. Arnold, A.A. Viggiano, R.A. Morris, "Rate Constants and Product Branching Fractions for the Reactions of  $\text{H}_3\text{O}^+$  and  $\text{NO}^+$  with  $\text{C}_2\text{-C}_{12}$  Alkanes," J. Phys. Chem. A, 102, pp8881-8887, 1998.
16. S.T. Arnold, R.A. Morris, A.A. Viggiano, "Reactions of  $\text{O}^-$  with Various Alkanes: Competition between Hydrogen Abstraction and Reactive Detachment," J. Phys. Chem. A, 102, pp1345-1348, 1998.
17. S.T. Arnold, S. Williams, Itzhak Doton, A.J. Midey, R.A. Morris, A.A. Viggiano, "Flow Tube Studies of Benzene Charge Transfer Reactions from 250 to 1400 K," J. Phys. Chem. A, 103, pp8421-8432, 1999.
18. S.T. Arnold, J.V. Seeley, J.S. Williamson, P.L. Mundis, A.A. Viggiano, "New Apparatus for the Study of Ion-Molecule Reactions at Very High Pressure (25-700 Torr): A Turbulent Ion Flow Tube (TIFT) study of Reactions of  $\text{SF}_6^- + \text{SO}_2$ ," J. Phys. Chem. A, 104, pp5511-5516, 2000.
19. M.S.B. Munson and F.H. Field, "Chemical Ionization Mass Spectrometry," J. Am. Chem. Soc., 88, pp2621-2630, 1966.
20. P.T. Palmer, T.F. Limero, "Mass Spectrometry in the U.S. Space Program: Past, Present, and Future," Am. Soc. For Mass Spectrometry, 12, pp656-675, 2001.
21. R.S. Houk, V.A. Fassel, G.D. Flesch, H.J. Svec, A.L. Gray, C.E. Taylor, "Inductively Coupled Argon Plasma as an Ion Source for Mass Spectrometric Determination of Trace Elements," Analytical Chemistry, 52, pp2283-2289, 1980.

## BIOGRAPHICAL SKETCH

Jayanth Pothireddy was born in India on March 14, 1977. He grew up in the town of Porumamilla and completed his schooling in 1992 from Vasista School, Madanapalle. He finished his high school studies from Vani Junior College, in 1994. Jayanth graduated from RV College of Engineering, Bangalore University, in 1999 where he obtained a Bachelor of Engineering in mechanical engineering. He pursued graduate studies at the University of Florida from 2001 to 2003 and obtained a Master of Science degree from the Department of Mechanical and Aerospace Engineering.